

# Experimental results on metamaterial simulation using SRR-loaded waveguides

J.D. Baena<sup>1</sup>, R. Marqués<sup>1,\*</sup>, J. Martel<sup>2</sup>, and F. Medina<sup>1</sup>

<sup>1</sup>Dept. de Electrónica y Electromagnetismo. Universidad de Sevilla. 41012 Sevilla, Spain

<sup>2</sup>Dept. de Física Aplicada II. Universidad de Sevilla, 41012 Sevilla, Spain

## Abstract

The recently proposed Split Ring Resonator (SRR) – loaded waveguide as a simulator of a left-handed medium (LHM) is extended to the simulation of negative magnetic permeability media (NMPM) and used for the study of wave propagation in these media. The experimental results are compared with those provided by the discrete metamaterial (LHM and NMPM) theory. Good qualitative and acceptable quantitative agreement has been found between theory and experiments.

## I. INTRODUCTION

Until now the experimental studies on NMPM and LHM have been centered on the measurement of the predicted left-handed passband [1] – [4], or on the qualitative demonstration of the negative refractive index [5]. As far as we know, other key properties of these media, such as attenuation constant, phase velocity and group velocity have not yet been measured. Recently, some of the authors have presented a one-dimensional simulation for left-handed media [3], consisting of a square SRR-loaded waveguide (SSLW). In the present work this device is extended to the simulation of both NMPM and LHM, and used for the analysis of wave propagation in these media. The obtained results are compared with those provided by the theory [6], [7].

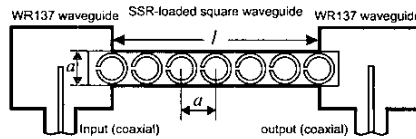


Fig. 1. Experimental setup (dimensions of the BC-SRR are the same as in [5]).

## II. EXPERIMENT

The experimental setup is shown in Fig.1. Two coaxial to rectangular waveguide transitions are connected to a rectangular SRR-loaded waveguide. No attempt to match these waveguides was made. For LHM simulations the SRR-loaded waveguide was a  $6 \times 6 \text{ mm}^2$  SSLW [3], [4]. The isotropic Broadside-coupled SRRs (BC-SRRs) [4], [6], with resonance frequency at 5.45 GHz, were used for loading the SSLW. Three different SSLW sections with a length of 6 cm were fabricated. These three sections were combined in all forms to give several SSLW sections with 6, 12 and 18 cm, which account for 10, 20 and 30 unit cells of the LHM, respectively. As is expected, the experimental results for the three lengths of SSLW show a very similar passband (see Fig.2), well below the cutoff

frequency of the hollow waveguide (25 GHz). In addition, a 6 cm long rectangular SRR-loaded waveguide (RSLW) of 6 mm height and 30 mm width was also fabricated and loaded by 5 equally spaced rows of 10 BC-SRRs. When the transmission through this  $30 \times 6 \text{ mm}^2$  RSLW is analyzed using the experimental setup of Fig.1, a rejection band appears at the location of the SSLW passband (see Fig.2.b). According to metamaterial theory [1], this rejection band should coincide with the region of negative magnetic permeability of the NMPM filling the rectangular waveguide (which is above cutoff). This coincidence between both frequency bands is a new confirmation of the theory reported in [3]. Of particular interest is the coincidence of the ends of both bands, at the frequency where the magnetic permeability vanishes for both the NMPM filling the RSLW and the LHM simulated by the SSLW. At low frequencies, the NMPM rejection band extends below the lower limit of the LHM passband. This fact can be explained by the presence of a region of high absorption and anomalous dispersion at these frequencies.

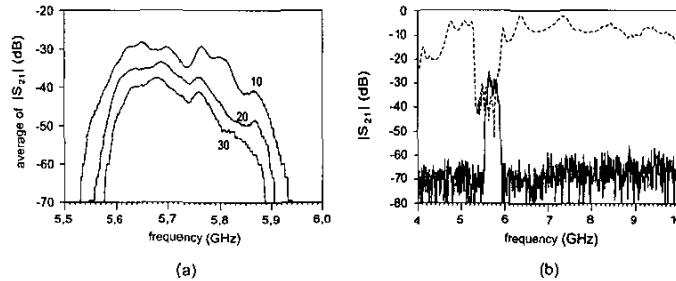


Fig. 2. (a) Measured  $|S_{21}|$  for three lengths of SSLW with 10, 20 and 30 unit cells. (b) Solid lines:  $|S_{21}|$  for a 6 cm long section of SSLW. Dashed lines:  $|S_{21}|$  for a 6 cm long section of a  $30 \times 6 \text{ mm}^2$  RSLW loaded with 5 equally spaced rows of SRRs.

The averages of the measured  $|S_{21}|$  values for each length of SSLW are shown in Fig.2.a. A quasi-uniform exponential decrease in the  $|S_{21}|$  can be observed. This decrease is consistent with the hypothesis of a simulated continuous medium with a frequency dependent attenuation constant. The attenuation constant computed from the aforementioned results for the  $|S_{21}|$  is shown in Fig.3.a. It was obtained by adjusting to the best slope the results for the  $|S_{21}|$  obtained for different SSLW lengths. Two sets of lengths were used for this purpose: the first one only consider sections with 20 and 30 unit cells, and the second one 10, 20 and 30 unit cells. A reasonable agreement between both sets of results is observed in Fig.3.a, except for the peak at 5.8 GHz. Since this peak is smaller for the calculations made with the longer SSLW sections, it seems to be related to the finite size of the SSLWs. In fact, this peak can be due to the influence of multiple reflections (which are neglected in our computations) in the shortest SSLW section. In view of the obtained values for the attenuation constant, these multiple reflections will not be completely attenuated in this SSLW section, thus affecting to the computed values of the attenuation constant. It is expected that LHM sim-

ulations with longer SSLW sections will give more accurate evaluations of this parameter. Work is in progress on this topic.

The experimental slow wave factor of a 10 and a 30 unit cells long SSLW sections are shown in Fig.3.b. This factor is defined as the ratio between the time delay for each SSLW section and the transit time of light over its length. From Fig.3.b it can be seen that the SSLW sections behave as delay lines. For long SSLW sections the phase shift at the transitions can be neglected in comparison with the phase shift through the SSLW. Thus, the aforementioned slow wave factor gives the inverse of the normalized group velocity of the LHM,  $c/v_g$ . This hypothesis is confirmed by the very similar slow wave factors observed in Fig.3.b for both SSLW sections. The ripples that appear in the 10 unit cells SSLW section almost disappear in the 30 unit cells SSLW section. Thus they can be attributed again to the effect of multiple reflections in the former SSLW section.

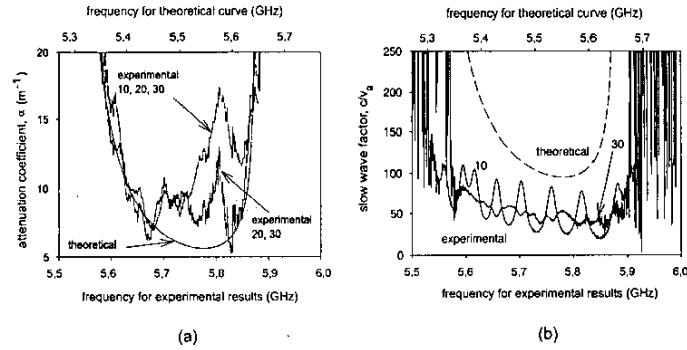


Fig. 3. (a) Measured and theoretical values for the attenuation constant along the SLW. (b) Measured and theoretical values for the slow wave factor  $c/v_g$ . Notice that the frequency scale for the theoretical data (upper scale) has been shifted so as both the theoretical and the experimental passbands are centered in the figure.

### III. THEORY

In two previous papers [6], [7] some of the authors presented an approximate analytical model for the simulated discrete NMPM and LHM. For the proposed structure this model assumes that the permittivity of the LHM is given by the negative effective permittivity of the square waveguide below cutoff [3],  $\epsilon = \epsilon_0 \left\{ 1 - \left( \frac{\omega_c}{\omega} \right)^2 \right\}$  where  $\omega_c$  is the cutoff frequency of the hollow waveguide. The NMPM and the LHM magnetic permeability is obtained as a function of the quasi-static magnetic polarizability of the BC-SRR, by using a local field theory. This polarizability is obtained as a function of the quasi static parameters of the BC-SRR (inductance, resistance and mutual capacitance). The ring resistance accounts for the ohmic losses in the rings, which determine the attenuation

constant in the proposed theory. The results provided by this theory are tested against the experimental results in Fig.3 (a) and (b). Except for a shift of less than 4% in the central frequency of the LHM passband (notice the different frequency scales in the figures), both set of results show a reasonable agreement. As was mentioned above, discrepancies in the attenuation constant can be due to the finite size of the samples and is expected that disappear if longer SSLW were used in the experiments. Discrepancies in the group velocity can be due to the capacitive loading of the SSLW associated to the SRRs, not taken into account in the model. This capacitive loading will cause an increase in the effective dielectric constant of the SSLW and, subsequently, a decrease in the cutoff frequency of this waveguide (this fact has been observed experimentally). This increase in the LHM effective dielectric constant results in a decrease of its absolute value. This decrease would explain the observed increase in the LHM group velocity (and subsequently the decrease of the delay time with respect to the theoretical predictions). More theoretical and experimental work on this topic is in progress.

#### IV. CONCLUSIONS

By comparing the experimental and theoretical results it can be concluded that the propagation of electromagnetic waves through SRR-loaded waveguides can be understood by means of the metamaterial theory developed in the reported references. Most of the predictions of this theory regarding bandwidth and central frequency of the pass- and rejection bands, as well as attenuation and group velocity in the passband, have been shown to be in qualitative and quantitative agreement with the experiments. However, some quantitative disagreements with the reported experiments still appear. These disagreements could be explained by the finite size of the waveguide sections and by other physical effects not taken into account in the model, such as non resonant capacitive couplings along the waveguide. More theoretical and experimental work on these topics is in progress. Applications in the design of waveguide pass- and rejection band filters, as well as delay lines, are expected in the future.

**Acknowledgement:** This work has been supported by the Spanish Ministry of Science and Technology and FEDER funds (project number TIC2001-3163).

#### REFERENCES

- [1] D.R. Smith, W.J. Padilla, D.C. Vier, S.C. Nemat-Nasser and S. Schultz, "Composite medium with simultaneously negative permability and permittivity," *Phys. Rev. Lett.*, Vol. 84, pp. 4184–4187, 2000
- [2] R.A. Shelby, D.R. Smith, S.C. Nemat-Nasser and S. Schultz, "Microwave transmission through a two-dimensional, isotropic, left-handed metamaterial," *Appl. Phys. Lett.*, Vol. 78, pp. 489–491, 2001.
- [3] R. Marqués, J. Martel, F. Mesa and F. Medina, "Left-handed media simulation and transmission of EM waves in subwavelength split-ring-resonator-loaded metallic waveguides" *Phys. Rev. Lett.*, vol. 89, pp. 13901(1-4), Oct. 2002.
- [4] R. Marqués, J. Martel, F. Mesa and F. Medina, "A new 2-D isotropic left-handed metamaterial design: theory and experiment," *Mic. and Opt. Tech. Lett.*, vol. 36, pp. 405–408, Dec. 2002.
- [5] R.A. Shelby, D.R. Smith and S. Schultz, "Experimental verification of a negative index of refraction," *Science*, Vol. 126, pp. 77–79, 2001.
- [6] R. Marqués, F. Medina and R. Rafi-El-Idrissi, "Role of bianisotropy in negative permeability and left-handed metamaterials" *Phys. Rev. B*, Vol. 65, 144440, 2002.
- [7] R. Marqués, F. Mesa, J. Martel and F. Medina, "Comparative analysis of edge- and broadside- coupled split ring resonators for metamaterial design. Theory and experiments," submitted to *IEEE Trans on Antennas and Prop.*